Magnetic Induction, Hall Current and Thermal Diffusion Effects on Unsteady MHD Nanofluif Flow Past an Oscillatory Semi-Infinite Vertical Flat Plate Embedded In A Porous Media

[1]Rhoda King'ali, [2]Mark Kimathi, [3]Benjamin Kikwai

[1]Mathematics & Statistics, Machakos University, Machakos, Kenya
[2]Mathematics & Statistics, Machakos University, Machakos, Kenya
[3]Mathematics & Statistics, Machakos University, Machakos, Kenya

Abstract: The effects of induced magnetic field, hall current and thermal diffusion for an incompressible, unsteady, viscous MHD Nano-fluid flow past a semi-infinite oscillating vertical flat plate embedded in a porous media, have been reported in this paper. A strong magnetic field is subjected transversely to the direction of the flow. The induced magnetic field is considered to be strong. The equations governing the flow, are solved by finite difference method of approximation and numerically solved by use of MATLAB software. The effects of the flow parameters on temperature, velocity, and concentration profiles, mass transfer and heat transfer have been investigated, discussed and results presented in graphs. The numerical results of this study reveal that; increasing the rotation parameter increases the induced magnetic field which in turn increases both primary and secondary velocities. Again, an increase the hall current parameter leads to an increase in both primary and secondary velocity profiles near the plate but the velocity remains constantly distributed far away from the plate.

Keywords: Chemical Reaction, Hall Effects, Induced Magnetic Field, MHD, Nanofluid, Rotation.

I. INTRODUCTION

MHD convective heat transfer in Nano-fluids has many applications and participates in an essential task in both sciences and engineering. They need heat transfer fluids in technology for applications such as cooling or heating, solar energy, and nuclear reactors, among others. Since fluids have a lower thermal conductivity than metals, it is essential to combine all types of fluids with Nano-sized metals to improve the fluids' heat transfer capacity. In this regard, the study of Nano-fluids has received extensive attention in the past decade due to enormous industrial, transportation, electronics, biomedical applications, such as in advanced nuclear systems, cylindrical heat pipes, automobiles, fuel cells, drug delivery, biological sensors, and hybrid-powered engines. Nano-fluid is a term initially used by [1] and refers to a new class of heat transfer fluids with superior thermal properties. The mixture of the base fluid and nanoparticles having unique physical and chemical properties is referred to as a Nano-fluid. It is expected that the presence of the nanoparticles in the Nano-fluid increases the thermal conductivity and therefore substantially enhances the heat transfer characteristics of the Nano-fluid. Thermal diffusion on free convection has become more significant due to its numerous applications in the engineering process and physics, more specifically in the design of high temperature processes, pertinent equipment, and space technology. Recent advancements in gas turbines, hypersonic flights, nuclear reactors, space vehicles, and nuclear power plants have attracted attention of scholars to research in this field. [2] studied hall effects on an unsteady magneto-hydrodynamic (MHD)

free convective flow of a viscous incompressible electrically conducting optically thick radiating fluid past a vertical porous plate in the presence of a uniform transverse magnetic field. [3] Studied on the effects of Hall current, rotation and Soret effects on MHD free convection heat and mass transfer flow past an accelerated vertical plate through a porous medium and considered magnetic Reynolds number so small such that the induced magnetic field can be neglected. [4] Studied the impact of Hall current, Radiation, Soret, and Dufour on an unsteady MHD Natural convective flow over an infinite vertical plate fixed in a porous media. They used efficient Galerkin method to solve the non-dimensional governing equations along with the boundary conditions. [5] Researched on the Hall current and thermo-diffusion effects on magneto-hydrodynamic convective flow near an oscillatory plate with ramped type thermal and solutal boundary conditions. [6] Studied ion slip and hall impacts on an unsteady laminar MHD convective rotating flow of heat generation of second grade fluid over a semi-infinite vertical moving permeable surface. [7] Researched on the Dufour, radiation absorption, Hall and ion slip effects on MHD free convective rotating flow of Ag - water based Nano-fluid past a semi -infinite permeable moving plate with constant heat source. [8] Studied thermo-diffusion, thermal radiation, Hall and ion slip effects on heat and mass transport of free convective MHD micro polar fluid flow bounded by a semi-infinite absorbent plate with rotation and suction. The plate was assumed to oscillate in time with constant frequency so that the solutions of the boundary layer are of the same oscillatory type. [9] Investigated on the Influence of Hall current and thermal diffusion on radiative hydro-magnetic flow of a rotating fluid in presence of heat absorption. [10] Studied radiation-absorption, chemical reaction, and Hall and ion-slip impacts on unsteady MHD free convective laminar flow of an incompressible viscous, electrically conducting and heat generation /absorbing fluid enclosed with a semi-infinite porous plate within a rotating frame. [8] Investigated on diffusion-thermo, radiation-absorption and Hall and ion slip effects on MHD free convective rotating flow of Nano-fluids (Ag and TiO_2) past a semi-infinite permeable moving plate with constant heat source. Most studies which have been done revolve on hall and ion slip effects with an exclusion of induced magnetic field.

Motivated by the above referenced work, the analysis of the effects of induced magnetic field, Hall current and thermal diffusion effects on water-based aluminum oxide have received little attention.

II. MATHEMATICAL FORMULATION

This study considers free convective and radiative magneto hydrodynamic fluid flow past an oscillating semi-infinite vertical porous plate subjected to a uniform magnetic field. The *x*-axis is at the vertically upward direction which is the direction of flow. The *z*-axis is taken normal to the plate and the velocity is a function of z and t; for z=0.
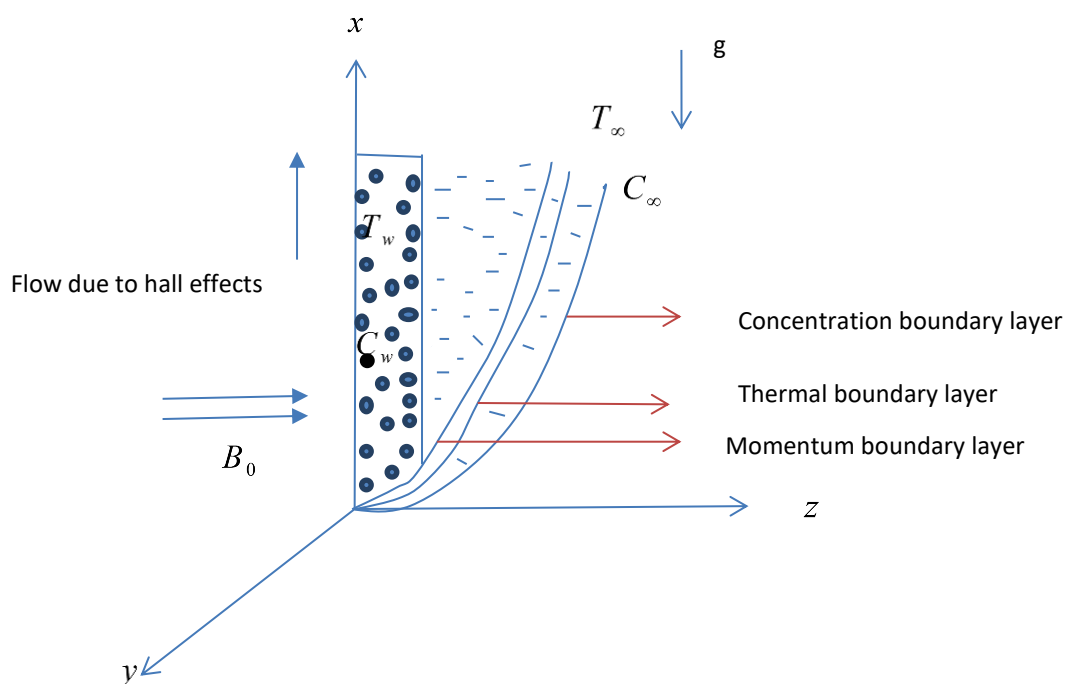

Fig. 1. Flow Geometry

MODEL ASSUMPTIONS

- The Nano-fluid is incompressible hence the density is assumed to be constant.

- The fluid flow is one-dimensional (1-D).

- Lorentz and gravitational forces are the only significant body forces.

- Since the flow is in presence of a strong applied magnetic field, the nano-fluid is considered electrically conducting.

- The flow is laminar; the fluid particles move in small layers.

- The chemical reaction between the fluid and nanoparticles is negligible

- Thermal conductivity, electrical conductivity and co-efficient of viscosity are constants.

- All variables are functions of $z \ and \ t$ only.

MODEL EQUATIONS

$$\frac{\partial w}{\partial z} = 0 \tag{1}$$

Applying Boussinesq approximation and considering the oscillatory motion given by [11] as well as neglecting the pressure gradient, and that the fluid velocity through porous media is approximately inversely proportional to the kinematic viscosity of the fluid , μ_{nf} , the momentum equations are given as;

$$\rho_{nf}\left[\frac{\partial v}{\partial t} + \frac{\partial u}{\partial z} - 2\Omega v\right] = \mu_{nf}\left[\frac{\partial^2 u}{\partial z^2}\right] - \frac{\mu_{nf}}{k}u + g\rho_{nf}\left[(\beta_T)_{nf}(T - T_\infty) + (\beta_C)_{nf}(C - C_\infty)\right]$$
$$+ B_0\vec{J}_y \tag{2}$$

$$\rho_{nf}\left[\frac{\partial v}{\partial t} + \frac{\partial v}{\partial z} - 2\Omega u\right] = \mu_{nf}\left[\frac{\partial^2 v}{\partial z^2}\right] - \frac{\mu_{nf}}{k}v + g\rho_{nf}\left[(\beta_T)_{nf}(T - T_\infty) + (\beta_C)_{nf}(C - C_\infty)\right]$$
$$+ bJ_Z - B_0\vec{J}_x \tag{3}$$

The boundary and initial conditions are specified as;

$For \ t \le 0; \ u = v = 0; \ T = T_\infty; \ C = C_\infty \ \ for \ \ all \ z$

$At \ t > 0 and \ z = 0; \ v = 0; u = U_r(1 + \varepsilon \cos t); \frac{\partial T}{\partial z} = -\frac{h_f}{k_{nf}}(T_w - T_\infty); \frac{\partial C}{\partial z} = -\frac{h_s}{D_B}(C_w - C_\infty)T = T_\infty;$

$For \ t > 0; \ u \to 0, v \to 0; \ T \to T_\infty; \ C \to C_\infty \ \ as \ z \to \infty$

Where ε is a small constant quantity and U_r is the uniform velocity.

However the strength of magnetic field is taken to be very large and the generalized Ohm's law is adapted with Hall impacts incorporated, therefore;

$$J + \frac{w_e\tau_e}{B_0}[J \times B] = \sigma\left[E + V \times B + \frac{1}{e\eta_e}\vec{\nabla}\rho_e\right] \tag{4}$$

ISSN 2394-9716

International Journal of Novel Research in Interdisciplinary Studies
Vol. 10, Issue 2, pp: (16-31), Month: March – April 2023, Available at: www.noveltyjournals.com

Since there are no externally applied electric field that is; $\vec{E} = 0$ and neglecting the electronic pressure; $\dfrac{1}{e\eta_e}\vec{\nabla}\rho_e = 0$

equation (4) becomes;

$$J + \frac{w_e\tau_e}{B_0}\left[J \times B\right] = \sigma\left[V \times B\right] \tag{5}$$

Where;

$$J = J_x i + J_y j + J k \quad and \quad \vec{B} = bi + 0j + B_0 k \text{ and } \vec{V} = ui + vj + wk \tag{6}$$

Taking into account the fore-mentioned assumptions equation (5) reduces to;

$$J_x + mJ_y = \delta B_0 v \tag{7}$$

$$\left(1 + \frac{m^2 b^2}{B_0^{\,2}}\right)J_y - mJ_x = \delta bw + \frac{\delta m b^2 v}{B_0} - \delta B_0 u \tag{8}$$

$$J_z - \frac{mb}{B_0}J_y = -\delta bv \tag{9}$$

Where; $m = w_e\tau_e$ is the hall current parameter and b is the induced magnetic field happening along the $x - axis$. Solving (7), (8) and (9) simultaneously, we yields;

$$J_x = \frac{\delta B_0}{1 + m^2 + \dfrac{m^2 b^2}{B_0^{\,2}}}\left(v + mu - \frac{mbw}{B_0}\right) \tag{10}$$

$$J_y = \frac{\delta B_0}{1 + m^2 + \dfrac{m^2 b^2}{B_0^{\,2}}}\left(mv - u + \frac{bw}{B_0} + \frac{mb^2 v}{B_0^{\,2}}\right) \tag{11}$$

$$J_z = \frac{\delta B_0}{1 + m^2 + \dfrac{m^2 b^2}{B_0^{\,2}}}\left(\frac{m^2 bv}{B_0} + \frac{mb^2 w}{B_0^{\,2}} + \frac{m^2 b^3 v}{B_0^{\,3}} - \frac{mbu}{B_0} - \frac{bv}{B_0}\right) \tag{12}$$

Substituting (10) to (12) into (2) and (3) we obtain;

$$\rho_{nf}\left\{\frac{\partial u}{\partial t} + w\frac{\partial u}{\partial z} - 2\Omega v\right\} = \mu_{nf}\left\{\frac{\partial^2 u}{\partial z^2}\right\} - \frac{\mu_{nf}}{k}u + g\rho_{nf}\left\{(\beta_T)_{nf}(T - T_\infty) + (\beta_C)_{nf}(C - C_\infty)\right\}$$

$$+ \frac{\delta B_0^{\,2}}{1 + m^2 + \dfrac{m^2 b^2}{B_0^{\,2}}}\left(mv - u + \frac{bw}{B_0} + \frac{mb^2 v}{B_0^{\,2}}\right) \tag{13}$$

ISSN 2394-9716

International Journal of Novel Research in Interdisciplinary Studies
Vol. 10, Issue 2, pp: (16-31), Month: March – April 2023, Available at: www.noveltyjournals.com

$$\rho_{nf}\left\{\frac{\partial v}{\partial t}+w\frac{\partial v}{\partial z}-2\Omega u\right\}=\mu_{nf}\left\{\frac{\partial^2 v}{\partial z^2}\right\}-\frac{\mu_{nf}}{k}v+g\rho_{nf}\left\{(\beta_T)_{nf}(T-T_\infty)+(\beta_C)_{nf}(C-C_\infty)\right\}$$

$$+\frac{\delta B_0^{\ 2}}{1+m^2+\frac{m^2 b^2}{B_0^{\ 2}}}\left(\begin{array}{c}\dfrac{m^2 b^2 v}{B_0^{\ 2}}-\dfrac{mb^2 u}{B_0^{\ 2}}-\dfrac{b^2 v}{B_0^{\ 2}}+\dfrac{mb^3 w}{B_0^{\ 3}}\\[2mm]+\dfrac{m^2 b^4 v}{B_0^{\ 4}}+\dfrac{mbw}{B_0}-mu-v\end{array}\right) \tag{14}$$

Considering, thermal radiation as the only significant energy source, S_e. However, the porous plate is in presence of thermal buoyancy effect with constant heat source and convective boundary condition.

According to [12] thermal diffusivity α_{nf} of nanofluid is given as; $\alpha_{nf}=\dfrac{k_{nf}}{(\rho C_p)_{nf}}$ hence equation reduces to;

$$\frac{\partial T}{\partial t}+w\frac{\partial T}{\partial z}=\alpha_{nf}\left(\frac{\partial^2 T}{\partial z^2}\right)+\frac{Q}{(\rho C_p)_{nf}}(T-T_\infty)-\frac{\partial q}{\partial z} \tag{15}$$

Where Q is temperature dependent volumetric rate of heat source. The radiative heat transfer is catered for by Stefan-Boltzmann law of radiation which advocates that the total radiative energy emitted by a black body is directly proportional to the fourth power of its temperature. From Rosseland approximation is given by, [13] the radiative heat flux is given as;

$$\frac{\partial q_r}{\partial z}=-\frac{16\sigma^* T_\infty^{\ 3}}{3k^*}\frac{\partial^2 T}{\partial z^2} \tag{16}$$

Where $\sigma^*(=5.67\times10^{-8}\ W/m^2 k^4)$ is the Stefan-Boltzmann constant and $k^*(m^{-1})$ is the Rosseland mean absorption coefficient.

$$\frac{\partial C}{\partial t}+w\frac{\partial C}{\partial z}=D_B\left(\frac{\partial^2 C}{\partial z^2}\right)+k'(C-C_\infty) \tag{17}$$

$$\frac{\partial b}{\partial t}=-v\frac{\partial b}{\partial z}-w\frac{\partial b}{\partial z}+B_0\frac{\partial u}{\partial z}+D_m\frac{\partial^2 b}{\partial z^2} \tag{18}$$

Nano-fluids possess various thermo-physical properties which include; electrical conductivity, specific heat capacity, , dynamic viscosity, density, thermal conductivity and coefficient of volume expansion due to changes in temperature and concentration. According to [13] the below are thermo-physical characteristics of nanofluids where f denote H_2O, s denote Al_2O_3 and ϕ is the solid volume fraction of the nanoparticles.

The density of the nanofluid is expressed as;

$$\rho_{nf}=(1-\phi)\rho_f+\phi\rho_s \tag{19}$$

The specific heat capacity of the Nano-fluid is expressed as;

$$(\rho C_P)_{nf}=(1-\phi)(\rho C_p)_f+\phi(\rho C_p)_s \tag{20}$$

ISSN 2394-9716

International Journal of Novel Research in Interdisciplinary Studies
Vol. 10, Issue 2, pp: (16-31), Month: March – April 2023, Available at: www.noveltyjournals.com

The thermal conductivity of the Nano-fluid is denoted as;

$$\frac{k_{nf}}{k_f} = \left[\frac{k_s + 2k_f - 2\phi(k_f - k_s)}{k_s + 2k_f + \phi(k_f - k_s)} \right] \qquad (21)$$

The dynamic viscosity of the Nano-fluid is expressed as;

$$\mu_{nf} = \frac{\mu_f}{(1-\phi)^{2.5}} \qquad (22)$$

The volume coefficient as a result of temperature changes of the Nano-fluid is expressed as;

$$(\beta_T)_{nf} = (1 - \phi_{Al_2O_3})(\beta_T)_{H_2O} + \phi_{Al_2O_3}(\beta_T)_{Al_2O_3} \qquad (23)$$

In a similar manner the volume expansion coefficient as a result of concentration change of the Nano-fluid is denoted as;

$$(\beta_C)_{nf} = (1 - \phi_{Al_2O_3})(\beta_C)_{H_2O} + \phi_{Al_2O_3}(\beta_C)_{Al_2O_3} \qquad (24)$$

Introducing the non-dimensional quantities;

$$u^* = \frac{u}{U_r}; \quad v^* = \frac{v}{U_r}; \quad z^* = \frac{z}{L}; \quad t^* = \frac{tU_r}{L}; \quad b^* = \frac{b}{B_0}$$

$$\psi = \frac{C - C_\infty}{C_w - C_\infty}; \quad \theta = \frac{T - T_\infty}{T_w - T_\infty}; \quad R = \frac{2\Omega v_f}{U_r^2}; \quad P_r = \frac{v_f}{\alpha_f}; \quad S = \frac{w_0}{U_r}; \quad K_r = \frac{Lk'}{U_r}$$

$$K = \frac{kU_r}{v_f L}; \quad Q_H = \frac{Qv_f^2}{U_r^2 k_f}; \quad M^2 = \frac{\delta_f B_0^2 L}{\rho_{nf} U_r}; \quad S_c = \frac{v}{D_B}; \quad G_r = \frac{\vec{g}(\beta_T)_{nf}(T_w - T_\infty)L}{U_r^2}$$

$$G_c = \frac{\vec{g}(\beta_C)_{nf}(C_w - C_\infty)L}{U_r^2} \quad R_m = \frac{U_r L}{D_m}, \quad R_e = \frac{U_r L}{v_f}$$

Where R is the Rotation parameter, S is the Suction parameter, P_r is the Prandtl number, K is the permeability parameter, M is the magnetic field parameter, Q_H is the heat source parameter, K_r is the chemically reacting parameter and S_c is the Schmidt's quantity, F is the thermic dissipation parameter, R_m is the magnetic Reynolds number, G_r and G_c are Grashof numbers and R_e is Reynolds number.

In this study, all the variables without superscript $\left(^*\right)$ star represent dimensional variables, otherwise non-dimensional variables.

According to [12] the continuity equation (1) reduces to;

$$w = w_0 \qquad (25)$$

Where w_0 is the normal velocity at the plate which is negative for suction and positive for injection.

Making use of the fore-mentioned non-dimensionalized quantities and nanoparticle thermo-physical characteristics,

ISSN 2394-9716

International Journal of Novel Research in Interdisciplinary Studies
Vol. 10, Issue 2, pp: (16-31), Month: March – April 2023, Available at: www.noveltyjournals.com

$$\left[1-\phi+\phi\left(\frac{\rho_s}{\rho_f}\right)\right]\left(\frac{\partial u^*}{\partial t^*}+S\frac{\partial u^*}{\partial z^*}-RR_e v^*\right)=\frac{1}{(1-\phi)^{2.5}}\frac{1}{R_e}\frac{\partial^2 u^*}{\partial z^{*2}}-\frac{1}{(1-\phi)^{2.5}}\frac{1}{K}u^*$$
$$+\left[1-\phi+\phi\left(\frac{\rho_s}{\rho_f}\right)\right](G_r\theta+G_c\psi)$$
$$+\left(1-\phi+\phi\left(\frac{\rho_s}{\rho_f}\right)\right)M^2\left(\frac{mv^*-u^*+mb^{*2}v^*}{1+m^2+m^2b^{*2}}\right)$$
$$-\left(1-\phi+\phi\left(\frac{\rho_s}{\rho_f}\right)\right)M^2S\left(\frac{b^*}{1+m^2+m^2b^{*2}}\right) \tag{26}$$

$$\left[1-\phi+\phi\left(\frac{\rho_s}{\rho_f}\right)\right]\left(\frac{\partial v^*}{\partial t^*}+S\frac{\partial v^*}{\partial z^*}-RR_e u^*\right)=\frac{1}{(1-\phi)^{2.5}}\frac{1}{R_e}\frac{\partial^2 v^*}{\partial z^{*2}}-\frac{1}{(1-\phi)^{2.5}}\frac{1}{K}v^*$$
$$+\left[1-\phi+\phi\left(\frac{\rho_s}{\rho_f}\right)\right](G_r\theta+G_c\psi)+\left(1-\phi+\phi\left(\frac{\rho_s}{\rho_f}\right)\right)$$
$$M^2\left(\frac{m^2b^{*2}v^*+m^2b^{*4}v^*-mb^{*2}u^*-b^{*2}v^*-v^*-mu^*}{1+m^2+m^2b^{*2}}\right)$$
$$-\left(1-\phi+\phi\left(\frac{\rho_s}{\rho_f}\right)\right)M^2S\left(\frac{mb^{*3}+mb^*}{1+m^2+m^2b^{*2}}\right) \tag{27}$$

$$\left[1-\phi+\phi\left(\frac{(\rho C_P)_s}{(\rho C_P)_f}\right)\right]\left(\frac{\partial\theta}{\partial t^*}+S\frac{\partial\theta}{\partial z^*}\right)=\frac{1}{P_r}\frac{1}{R_e}\frac{\partial^2\theta}{\partial z^{*2}}+Q_H\theta+\frac{4}{3}\frac{F}{R_e}\frac{\partial^2\theta}{\partial z^{*2}} \tag{28}$$

$$\frac{\partial\psi}{\partial t^*}+S\frac{\partial\psi}{\partial z^*}=\frac{1}{S_c}\frac{1}{R_e}\frac{\partial^2\psi}{\partial z^{*2}}+K_r\psi \tag{29}$$

$$\frac{\partial b^*}{\partial t^*}=S\frac{\partial b^*}{\partial z^*}+\frac{\partial u^*}{\partial z^*}+\frac{1}{R_e}\frac{\partial^2 b^*}{\partial z^{*2}} \tag{30}$$

For $t\le 0$; $u^*=v^*=0$; $\theta=0$; $\psi=0$ *for all* z

For $t>0$ *and* $z=0$; $u=U_r(1+\varepsilon\cos t)$; $v=0$, $\frac{\partial\theta}{\partial z^*}=-N_c(1-\theta(z))$, $\frac{\partial\psi}{\partial z^*}=-N_d(1-\psi(z))$

For $t>0$; $u=v=0$; $\theta\to 0$; $\psi\to 0$ *as* $Z\to\infty$

METHOD OF SOLUTION

Finite difference method is used to solve equations (22) to (26). This is because it converges to exact solution as the stepsize decreases, it is stable and consistent since the truncation error tends to zero as the step size decreases.

$$u_i^{*n+1} = \Delta t \left\{ \begin{array}{c} \dfrac{S\left[\dfrac{u_{k+1}^{*n} - u_{k-1}^{*n}}{2\Delta z}\right] + R v_{i,k}^{*n} + \dfrac{1}{(1-\phi)^{2.5}\left(1-\phi+\phi\left(\dfrac{\rho_s}{\rho_f}\right)\right)} \dfrac{1}{R_e}\left(\dfrac{u_{k+1}^{*n} - 2u_k^{*n} + u_{k-1}^{*n}}{(\Delta z)^2}\right) -}{\dfrac{1}{(1-\phi)^{2.5}\left(1-\phi+\phi\left(\dfrac{\rho_s}{\rho_f}\right)\right)} \dfrac{1}{K} u_{i,k}^{*n} + \left(G_r\theta_{i,k}^n + G_c\psi_{i,k}^n\right) +} \\[3em] M^2\left(\dfrac{m v_{i,k}^{*n} - u_{i,k}^{*n} + mb_{i,k}^{*2^n} v_{i,k}^{*n}}{1+m^2+m^2 b^{*2}}\right) - M^2 S\left(\dfrac{b_{i,k}^{*n}}{1+m^2+m^2 b_{i,k}^{*2^n}}\right) \end{array} \right\} + u_i^{*n} \qquad (31)$$

$$v_i^{*n+1} = \Delta t \left\{ \begin{array}{c} \dfrac{S\left[\dfrac{v_{k+1}^{*n} - v_{k-1}^{*n}}{2\Delta z}\right] + R u_{i,k}^{*n} + \dfrac{1}{(1-\phi)^{2.5}\left(1-\phi+\phi\left(\dfrac{\rho_s}{\rho_f}\right)\right)} \dfrac{1}{R_e}\left(\dfrac{v_{k+1}^{*n} - 2v_k^{*n} + v_{k-1}^{*n}}{(\Delta z)^2}\right) -}{\dfrac{1}{(1-\phi)^{2.5}\left(1-\phi+\phi\left(\dfrac{\rho_s}{\rho_f}\right)\right)} \dfrac{1}{K} v_{i,k}^{*n} + \left(G_r\theta_{i,k}^n + G_c\psi_{i,k}^n\right) +} \\[3em] M^2\left(\dfrac{m^2 b_{i,k}^{*2^n} v_{i,k}^{*n} + m^2 b_{i,k}^{*4^n} v_{i,k}^{*n} - mb_{i,k}^{*2^n} u_{i,k}^{*n} - b_{i,k}^{*2^n} v_{i,k}^{*n} - v_{i,k}^{*n} - mu_{i,k}^{*n}}{1+m^2+m^2 b^{*2}}\right) - \\[2em] M^2 S\left(\dfrac{mb_{i,k}^{*3^n} + mb_{i,k}^{*n}}{1+m^2+m^2 b_{i,k}^{*2^n}}\right) \end{array} \right\} + u_i^{*n} \qquad (32)$$

$$\theta_i^{n+1} = \Delta t \left\{ \begin{array}{c} S\left(\dfrac{\theta_{k+1}^n - \theta_{k-1}^n}{2\Delta z}\right) + \\[1.5em] \dfrac{1}{1-\phi+\phi\left(\dfrac{(\rho\beta)_s}{(\rho\beta)_f}\right)}\left[\dfrac{1}{P_r R_e}\left(\dfrac{\theta_{k+1}^n - 2\theta_k^n + \theta_{k-1}^n}{(\Delta z)^2}\right) + Q_H\theta_{i,k}^n + \dfrac{4}{3}\dfrac{F}{R_e}\left(\dfrac{\theta_{k+1}^n - 2\theta_k^n + \theta_{k-1}^n}{(\Delta z)^2}\right)\right] \end{array} \right\} + \theta_{i,k}^n \qquad (33)$$

$$\psi_i^{n+1} = \Delta t \left\{ S\left[\dfrac{\psi_{k+1}^n - \psi_{k-1}^n}{2\Delta z}\right] + \dfrac{1}{S_c R_e}\left[\dfrac{\psi_{k+1}^n - 2\psi_k^n + \psi_{k-1}^n}{(\Delta z)^2}\right] + K_r\psi_{i,k}^n \right\} + \psi_i^n \qquad (34)$$

$$b_i^{*n+1} = \Delta t \left\{ -v^*\left[\dfrac{b_{k+1}^{*n} - b_{k-1}^{*n}}{2\Delta z}\right] + S\left[\dfrac{b_{k+1}^{*n} - b_{k-1}^{*n}}{2\Delta z}\right] - \left[\dfrac{u_{k+1}^{*n} - u_{k-1}^{*n}}{2\Delta z}\right] + \dfrac{R_m}{R_e}\left[\dfrac{b_{k+1}^{*n} - 2b_k^{*n} + b_{k-1}^{*n}}{(\Delta z)^2}\right] \right\} + b_i^{*n} \qquad (35)$$

The dicretisized frontier conditions are;

$$For\ t \leq 0;\ u_{i,k}^{*n} = v_{i,k}^{*n} = 0;\ \theta_{i,k}^n = 0;\ \psi_{i,k}^n = 0\ \ for\ all\ k$$

![Novelty Journals]

ISSN 2394-9716

International Journal of Novel Research in Interdisciplinary Studies
Vol. 10, Issue 2, pp: (16-31), Month: March – April 2023, Available at: **www.noveltyjournals.com**

$For\ t > 0\ and\ k = 0;\ u^{*n}_{i,k} = U_r\left(1 + \varepsilon \cos t\right);\ v^{*n}_{i,k} = 0,$

$\theta^n_{k+1} = -N_c\left(1 - \theta^n_{i,k}\right)2\Delta z + \theta^n_{k=1},\ \psi^n_{k+1} = -N_d\left(1 - \psi^n_{i,k}\right)2\Delta z + \psi^n_{k-1}$

$For\ t > 0;\ u^{*n}_{i,k} = v^{*n}_{i,k} = 0;\ \theta^n_{i,k} \to 0;\ \psi^n_{i,k} \to 0\ \ as\ k \to \infty$

III.   RESULTS AND DISCUSSIONS

In this numerical work, the following parameter values have been used unless otherwise stated, $\phi = 0.35$, $\rho_s = 3950$, $\rho_f = 997$, $(C_p)_s = 765$, $(C_p)_f = 4179$, $R = 0.015$, $S = -0.2$, $K = 0.8$, $m = 0.7$, $M = 2$, $G_r = 1.5$, $G_c = 1.5$, $S_c = 0.8$, $K_r = 2$, $R_m = 65$, $R_e = 180$, $N_c = 1$, $N_d = 1$, $P_r = 6.72$, $Q_H = 2.5$, $F = 0.6$

i.   Effects of Flow Parameters on Velocity Profiles

Fig. 2. Variation of primary velocity with Magnetic Field Parameter, M

Fig. 3. Variation of Secondary velocity with magnetic field parameter, M
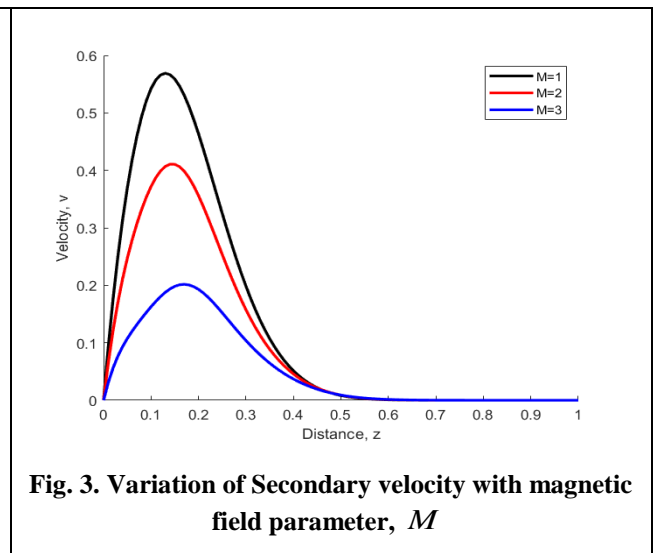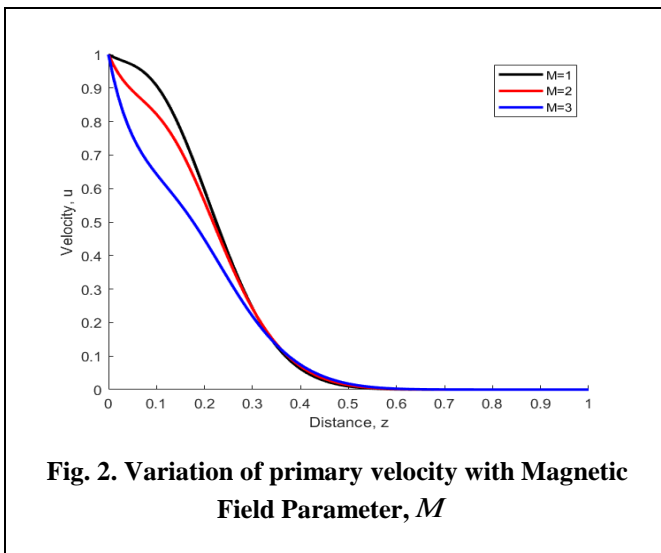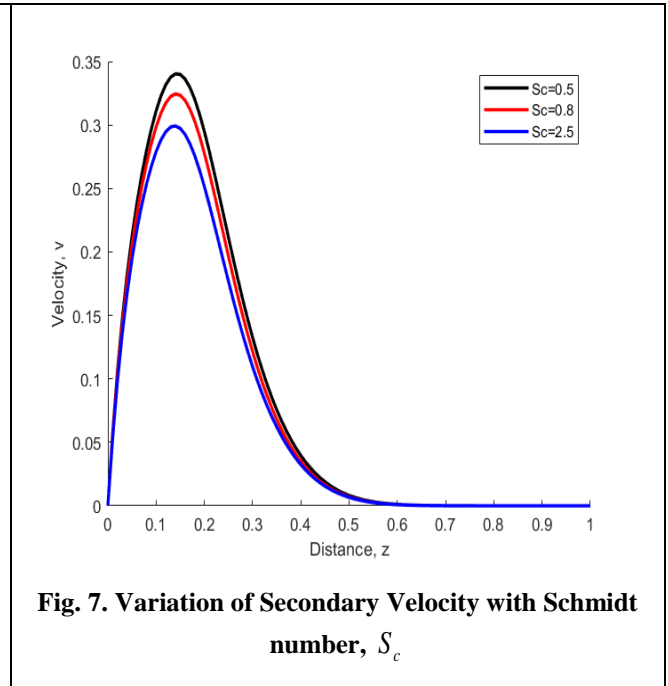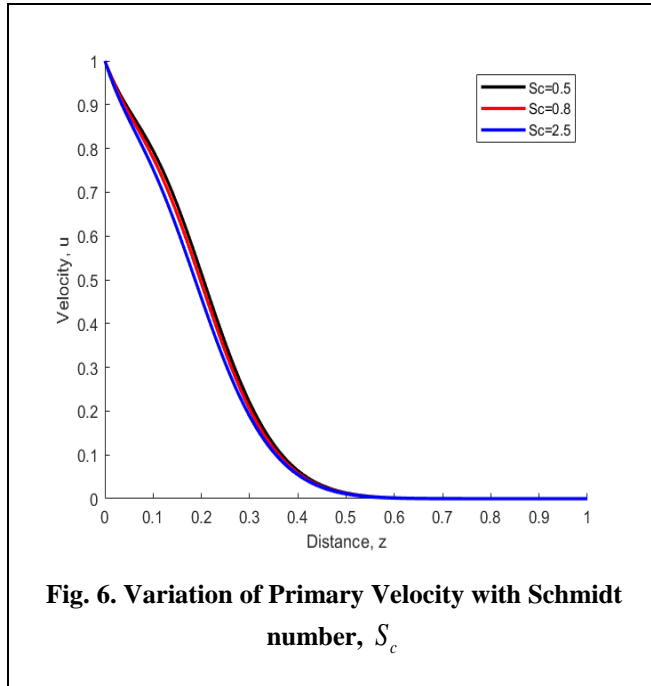
From Fig. 2 & 3, we note that;

An increase in the magnetic field parameter, M causes a decrease in both primary and secondary velocity profiles. This is because it increases Lorentz forces which creates a force opposed to the fluid motion.

Fig. 4. Variation of primary velocity with Reynolds Number, R_e

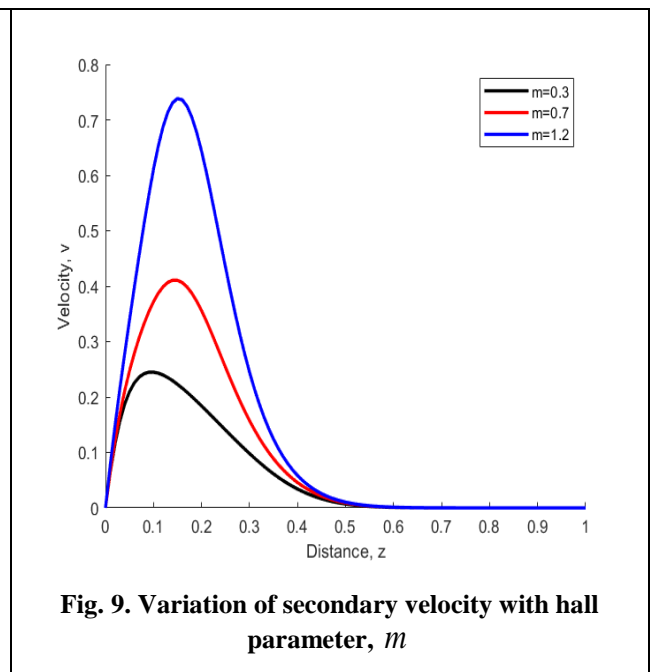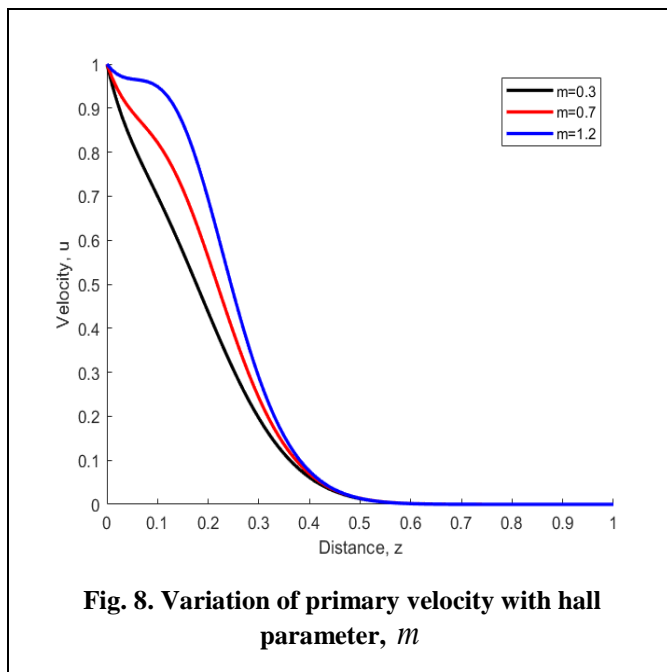**Fig. 5. Variation of Secondary velocity with Reynolds Number, R_e**
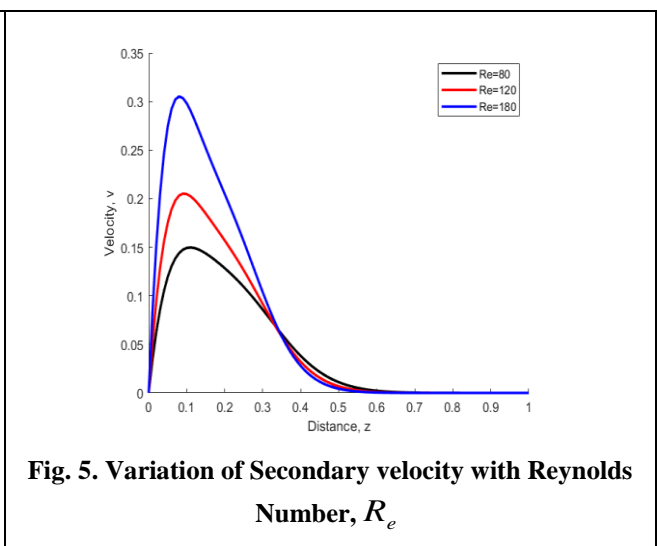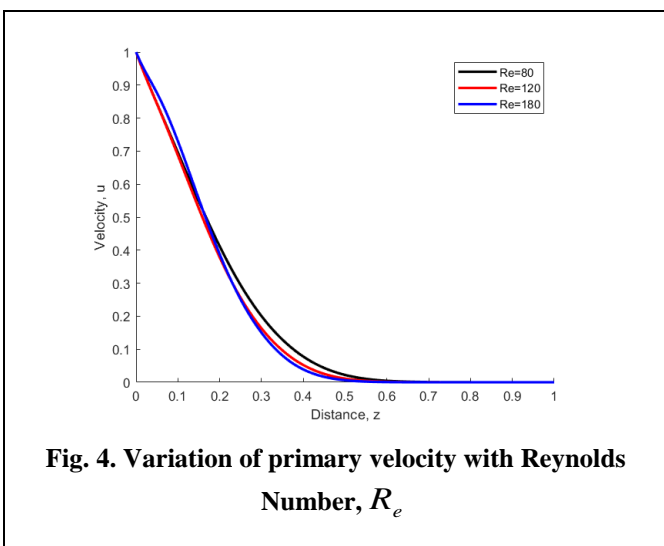
From Fig. 4 & 5, we observe that;

An increase in the Reynolds Number leads to an increase in both primary and secondary velocities near the plate but decreases the velocity away from the plate to a point where the velocity becomes uniformly distributed. This is because increase in Reynolds number means the viscous force becomes less predominant hence the inertia forces prevails.
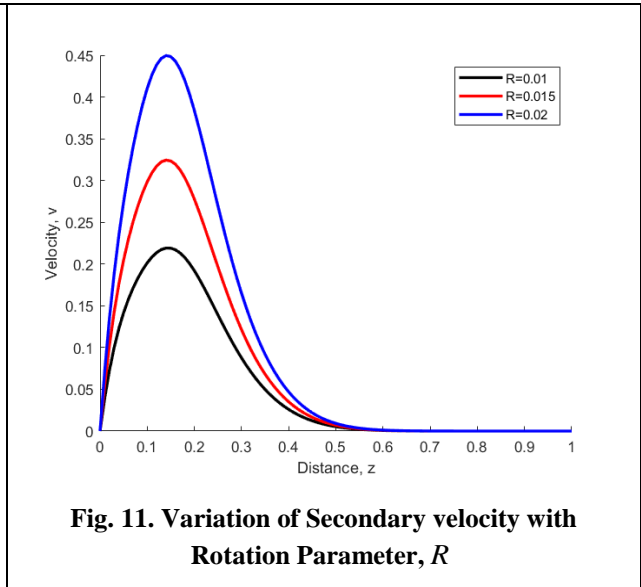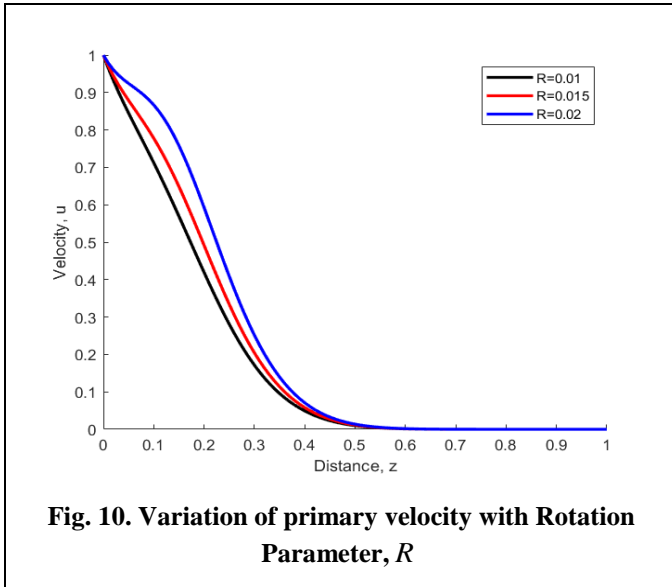

Fig. 6. Variation of Primary Velocity with Schmidt number, S_c

Fig. 7. Variation of Secondary Velocity with Schmidt number, S_c

From Fig. 6 & 7, it is noted that;

An increase in the mass diffusion parameter, S_c leads to a decrease in both primary and secondary velocity profiles near the plate and remain constantly distributed far away from the plate. This is due to increase in viscous diffusion rate which leads to decrease in buoyancy forces; which in turn results to reduction in flow of the fluid.

Fig. 8. Variation of primary velocity with hall parameter, m

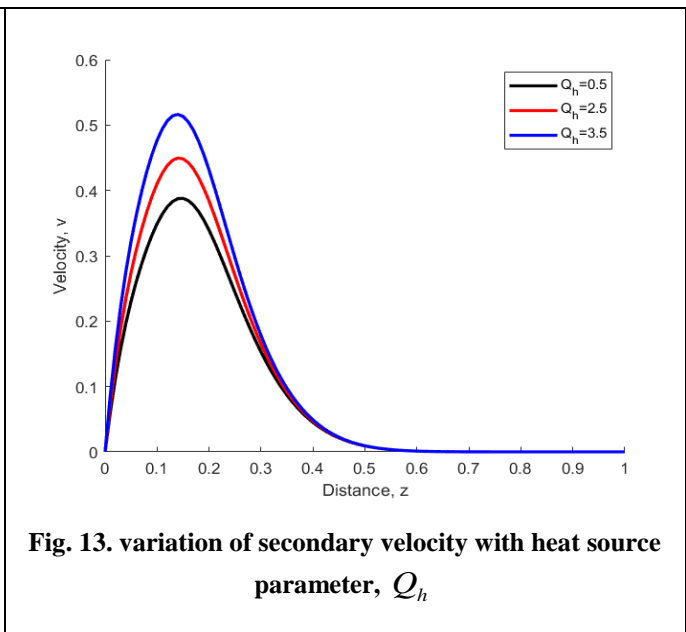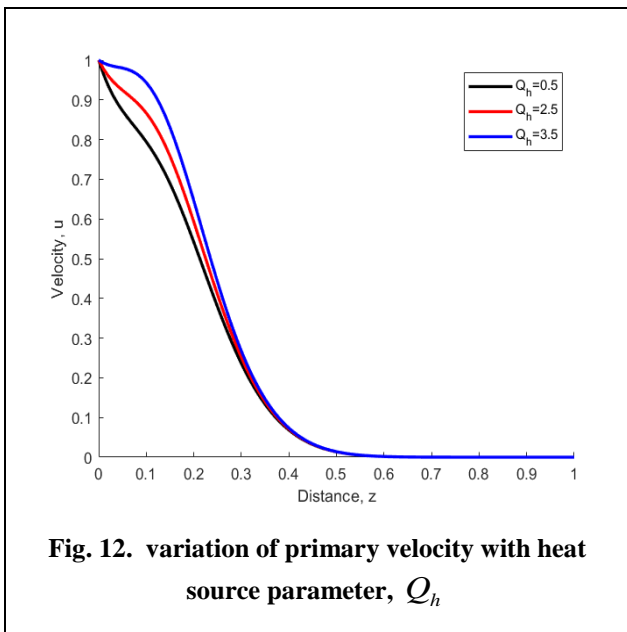**Fig. 9. Variation of secondary velocity with hall parameter, m**

From Fig 8 & 9, it is noted that;

An increase the hall current parameter leads to an increase in both primary and secondary velocity profiles near the plate but the velocity remains constantly distributed far away from the plate. This is as a result of the fact that increase in the hall parameter predominates Hall Effect on flow of electrons hence an increase in velocity profiles.
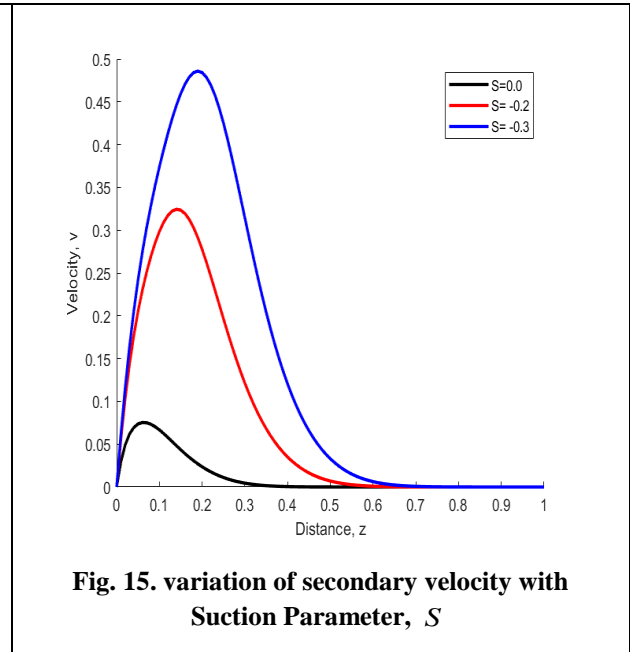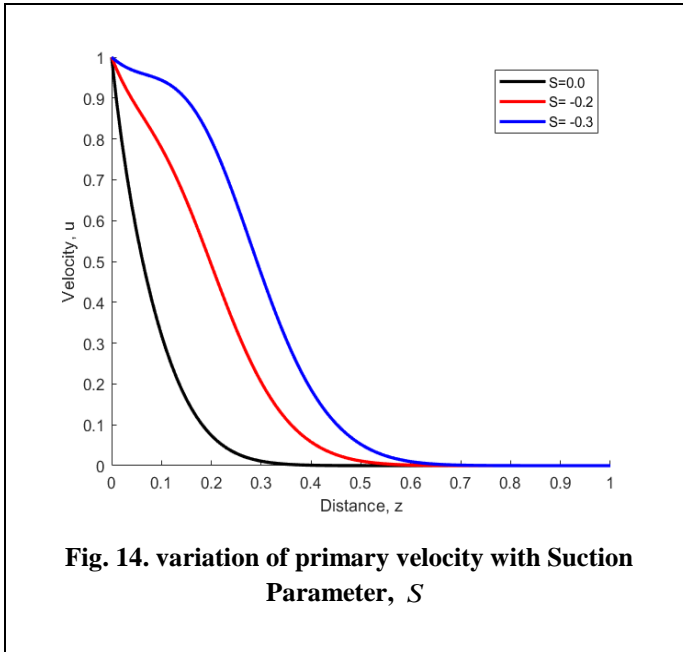

Fig. 10. Variation of primary velocity with Rotation Parameter, R

Fig. 11. Variation of Secondary velocity with Rotation Parameter, R

From Fig. 10 & 11, it is noted that;

Increase in the rotation parameter, R increases both primary and secondary velocities near the plate and remains constantly distributed far away from the plate. This is due to increase in Coriolis force on velocity of the rotating fluid hence increase in velocity.

Fig. 12. variation of primary velocity with heat source parameter, Q_h

Fig. 13. variation of secondary velocity with heat source parameter, Q_h

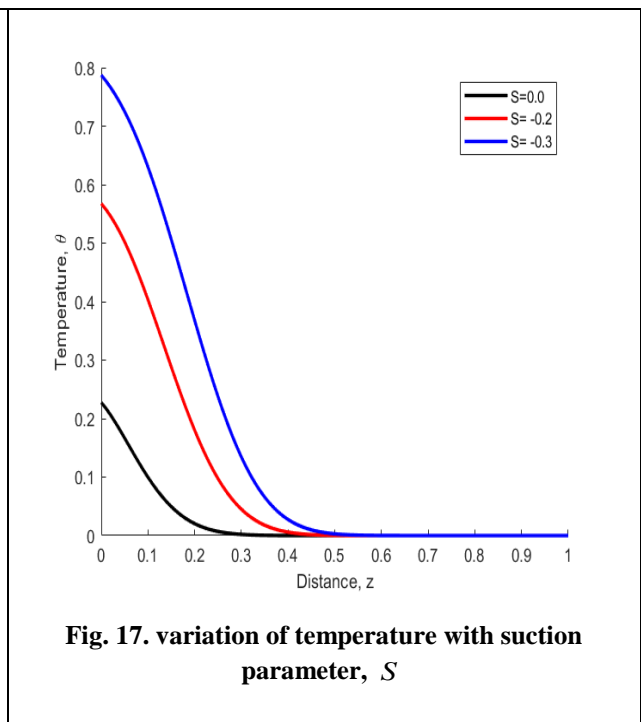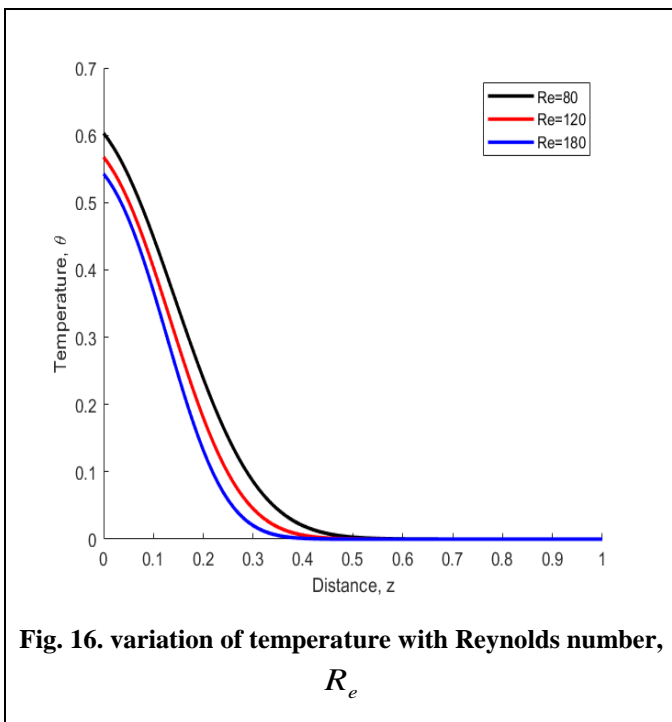From Fig. 12 & 13, it is observed that;

An increase in the heat source parameter, Q_h increases both primary and secondary velocities near the plate and remains constantly distributed far away from the plate. Increase in heat source means increase in temperature gradient and this leads to increase in velocity distributions.

Fig. 14. variation of primary velocity with Suction Parameter, S

Fig. 15. variation of secondary velocity with Suction Parameter, S
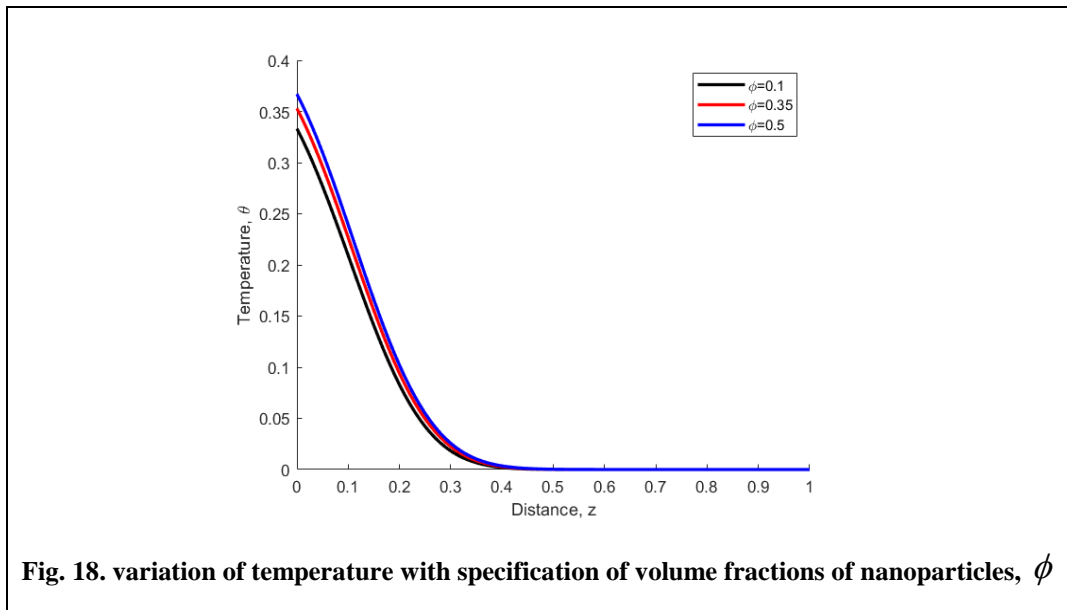
From Fig. 12 & 13, it is observed that;

Increase in the suction parameter increases both primary and secondary profiles near the plate and the velocities remain constant far away from the plate. This is because increase in suction leads to suction pressure which creates a low pressure region which makes the fluid to flow faster to fill the lower pressure region hence an increase velocity.

ii. Effects of Flow Parameter on Temperature Profiles

Fig. 16. variation of temperature with Reynolds number, R_e

Fig. 17. variation of temperature with suction parameter, S

Fig. 18. variation of temperature with specification of volume fractions of nanoparticles, ϕ
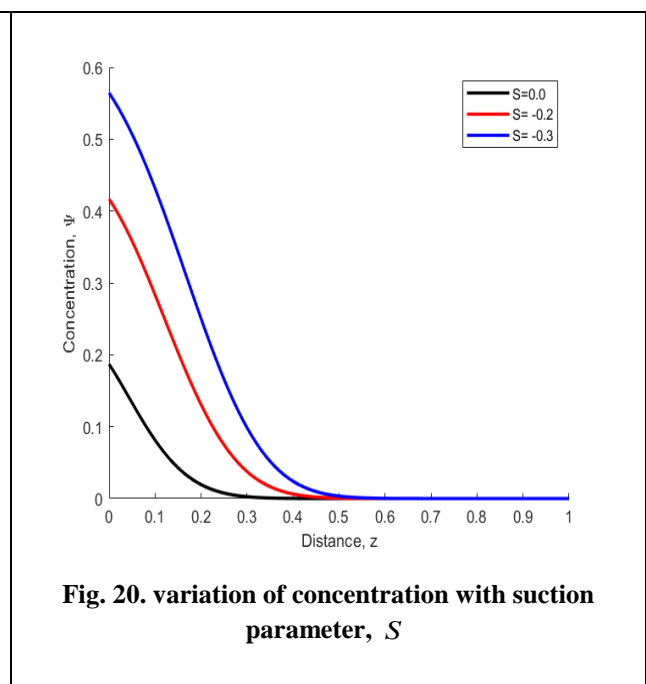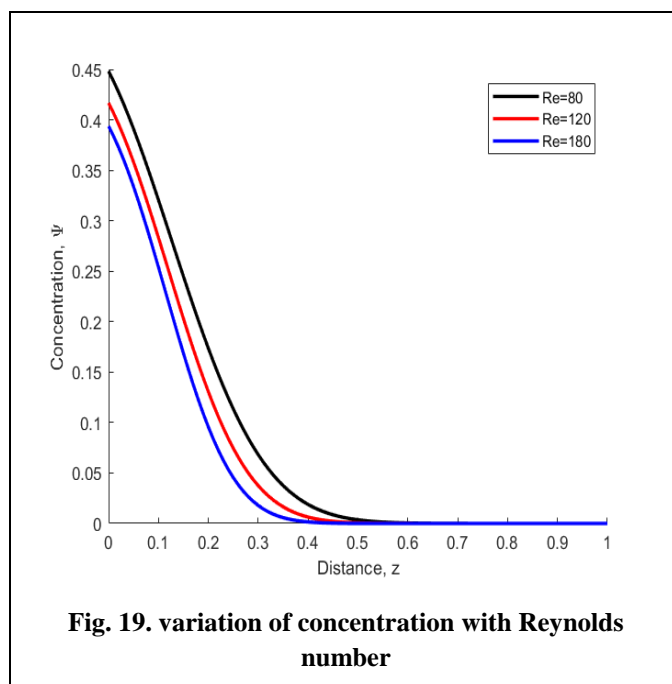
From Fig. 16, 17 & 18, it is note that;

- An increase in Reynolds number, R_e increases the temperature profiles. This is due to decrease in viscous forces and since temperature and viscosity are inversely proportional, a decrease in viscous forces yields an increase in temperature.

- A decrease in the suction parameter, S increases the temperature profiles. This is because suction leads to increase in velocities which further leads to the increase in the kinetic energy which is converted in to thermal energy and this results to temperature increase.

- Increasing the volume fractions of nanoparticles, ϕ causes an increase in the temperature profiles. This is as a result of increase in the thermal boundary layer thickness.

iii. Effects of Flow Parameters on Concentration Profiles

Fig. 19. variation of concentration with Reynolds number

Fig. 20. variation of concentration with suction parameter, S
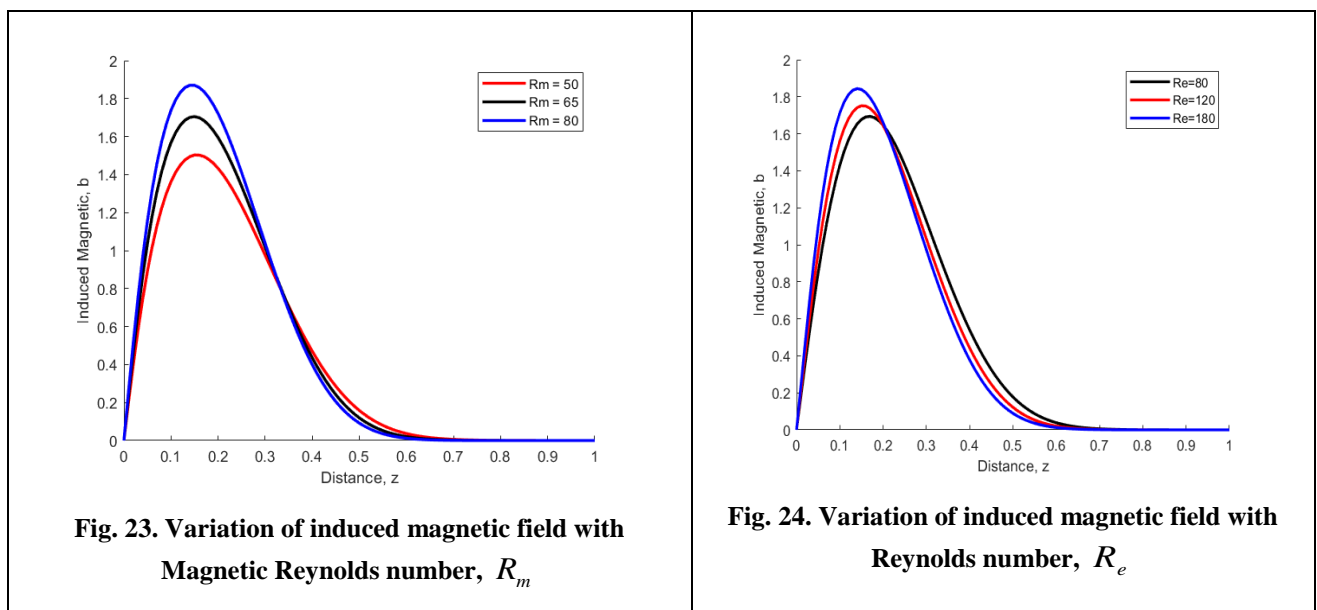
From Fig. 19 to 21, it is note that;

• An increase in the Reynolds number, R_e leads to a decrease in the concentration profiles due to increase in inertial forces which increases the velocity hence a decrease in concentration.

• Decreasing the suction parameter, S increases the concentration. This is due to high temperatures as a result of increased kinetic energy hence a decrease in concentration boundary layer.
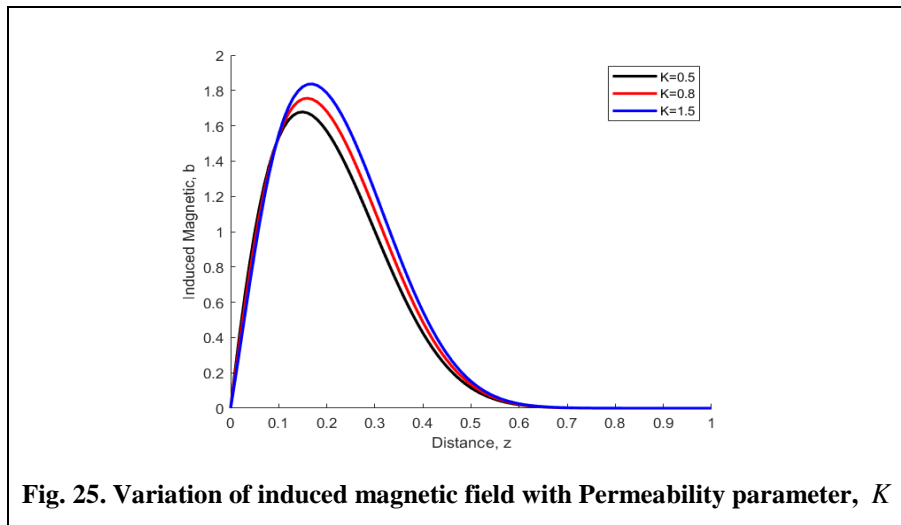
iv. Effects of Flow Parameters on induced magnetic field Profiles

Fig. 21. Variation of induced magnetic field with Magnetic Field

Fig. 22 variation of induced magnetic field with suction parameter, S
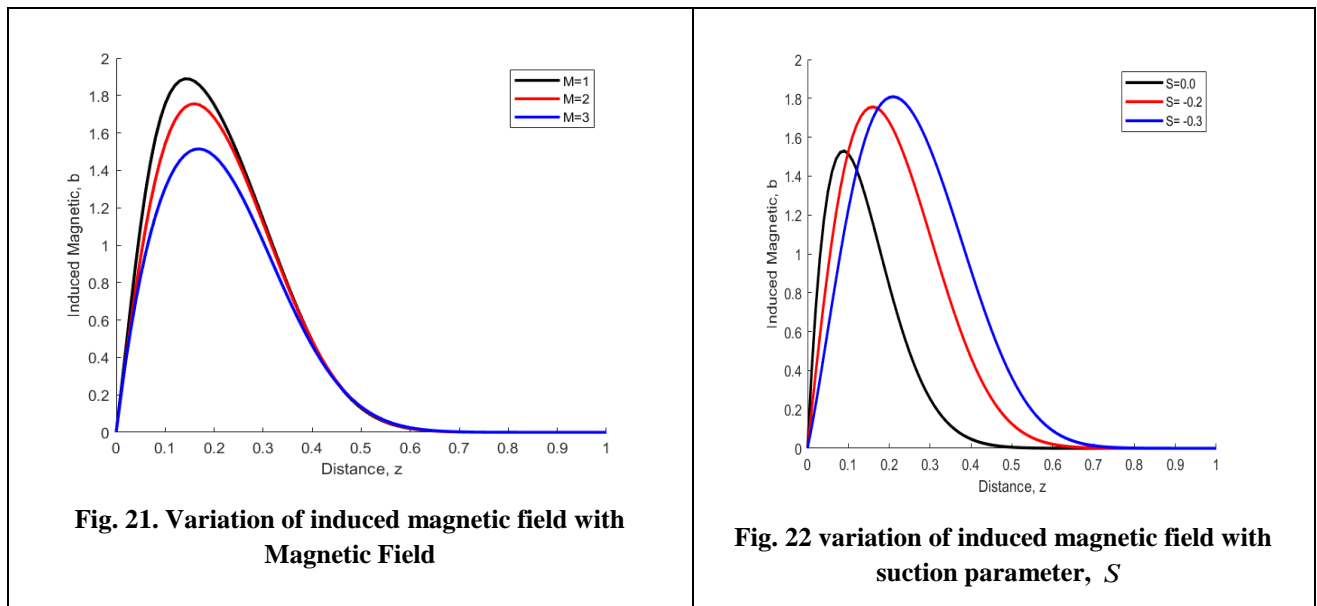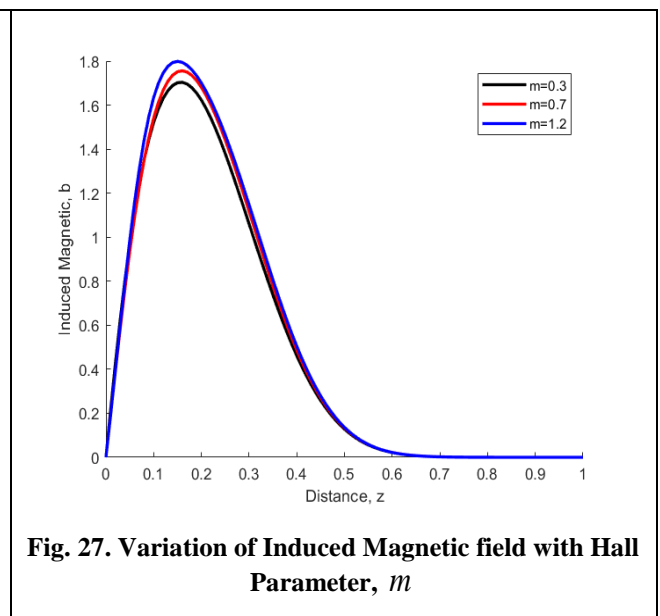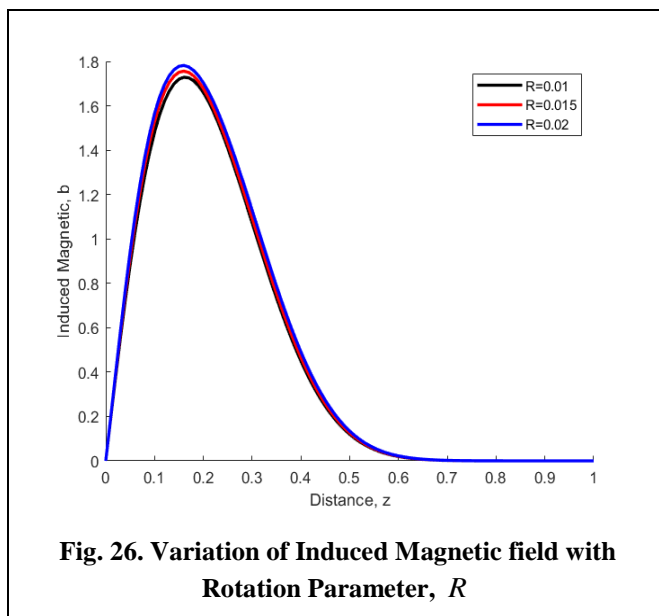
From Fig. 22 & 23, it is observed that;

• Increase in the magnetic field parameter reduces the induced magnetic field profiles. Increase in magnetic parameter leads to an increase in Lorentz forces which opposes the flow hence a decrease in the induced magnetic field.

• Reducing the Suction parameter diminishes the induced magnetic field profiles near the plate and increases the induced magnetic far away from the plate. This is because with decrease in suction parameter, the velocity decreases hence a decrease in interaction between the magnetic field and the fluid leading to a decreased magnetic induction.

Fig. 23. Variation of induced magnetic field with Magnetic Reynolds number, R_m

Fig. 24. Variation of induced magnetic field with Reynolds number, R_e

Fig. 25. Variation of induced magnetic field with Permeability parameter, K

From Fig. 24 to 26, it is observed that;

- An increase in the magnetic Reynolds number, R_m and Reynolds number causes an increase in the induced magnetic field near the plate and decreases the induced magnetic field far away from the plate. This is due to the fact that presence of magnetic field acting perpendicular to the flow in an electrically conducting fluid produces a force which acts against the fluid flow (figure 24 & 25)

- An increase in the Permeability parameter, K causes an increase in the induced magnetic field near the plate and decreases the induced magnetic field far away from the plate.

Fig. 26. Variation of Induced Magnetic field with Rotation Parameter, R

Fig. 27. Variation of Induced Magnetic field with Hall Parameter, m

From Fig. 27 & 28, it is observed that;

- The induced magnetic field increases with an increase in rotation parameter, R and hall parameter, m. This is as a result increased magnetic field which induces electromotive force hence the faster the rotation the greater the induced magnetic field.

- Increase in hall parameter, m leads to increase in induced magnetic field. This is due to increase in the hall parameter which predominates Hall Effect on flow of electrons which in turn increases magnetic field hence an increase in induced magnetic field.

IV. CONCLUSION

In this work the effects of induced magnetic field, hall current and thermal diffusion past a semi- infinite porous plate with an oscillatory motion have been formulated and solved numerically. The equations governing the flow have been solved by finite difference method and numerical results simulated using MATLAB software. It is found that increasing the rotation parameter increases the induced magnetic field which in turn increases both primary and secondary velocities. Again, an increase the hall current parameter leads to an increase in both primary and secondary velocity profiles near the plate but the velocity remains constantly distributed far away from the plate. However, an increase in suction parameter tends to increase temperature which in turn increases concentration.

From this observations, it's clear that the parameters in the governing equations affect velocity, temperature, concentration and induced magnetic profiles. It is recommended that this work can be extended by considering: variable strong magnetic field inclined at an angle to the plate, turbulent flow of nanofluid and also the effects of parameters in the governing equations on skin friction on both heat and mass transfer.

REFERENCES

[1] Choi, S. U., & Eastman, J. A. (1995). *Enhancing thermal conductivity of fluids with nanoparticles* (No. ANL/MSD/CP-84938; CONF-951135-29). Argonne National Lab.(ANL), Argonne, IL (United States).

[2] Das, S., Guchhait, S. K., Jana, R. N., & Makinde, O. D. (2016). Hall effects on an unsteady magneto-convection and radiative heat transfer past a porous plate. *Alexandria Engineering Journal*, *55*(2), 1321-1331.

[3] Sarma, D., & Pandit, K. K. (2018). Effects of Hall current, rotation and Soret effects on MHD free convection heat and mass transfer flow past an accelerated vertical plate through a porous medium. *Ain Shams Engineering Journal*, *9*(4), 631-646.

[4] Kumar, M. A., Reddy, Y. D., Goud, B. S., & Rao, V. S. (2021). Effects of soret, dufour, hall current and rotation on MHD natural convective heat and mass transfer flow past an accelerated vertical plate through a porous medium. *International Journal of Thermofluids*, *9*, 100061.

[5] Nandi, S., & Kumbhakar, B. (2021). Hall current and thermo-diffusion effects on magnetohydrodynamic convective flow near an oscillatory plate with ramped type thermal and solutal boundary conditions. *Indian Journal of Physics*, 1-14.

[6] Veera Krishna, M. (2020). Hall and Ion slip Effects on MHD Free Convective Rotating Flow Bounded by the Semi-infinite Vertical Porous Surface. *Heat Transfer*, *49*(4), 1920-1938.

[7] Dharmaiah, G., Baby Rani, C. H., Vedavathi, N., & Balamurugan, K. S. (2020). Hall and ion slip effects on Ag-water based MHD nanofluid flow over a semi-infinite vertical plate embedded in a porous medium. *Frontiers in Heat and Mass Transfer (FHMT)*, *14*.

[8] Krishna, M. V., & Chamkha, A. J. (2019). Hall and ion slip effects on MHD rotating boundary layer flow of nanofluid past an infinite vertical plate embedded in a porous medium. *Results in Physics*, *15*, 102652.

[9] Venkateswarlu, M., Makinde, O. D., & Reddy, P. R. (2019). Influence of Hall current and thermal diffusion on radiative hydromagnetic flow of a rotating fluid in presence of heat absorption. *Journal of Nanofluids*, *8*(4), 756-766.

[10] Krishna, M. V. (2021). Radiation-absorption, chemical reaction, Hall and ion slip impacts on magnetohydrodynamic free convective flow over semi-infinite moving absorbent surface. *Chinese Journal of Chemical Engineering*.

[11] Ganapathy, R. (1994). A note on oscillatory Couette flow in a rotating system.

[12] Das, K. (2014). Flow and heat transfer characteristics of nanofluids in a rotating frame. *Alexandria Engineering Journal*, *53*(3), 757–766.

[13] Veera Krishna, M., Ameer Ahamad, N., & Chamkha, A. J. (2021). Hall Effects on Unsteady Magnetohydrodynamic Flow of a Nanofluid Past an Oscillatory Vertical Rotating Flat Plate Embedded in Porous Media. *Journal of Nanofluids*, *10*(2), 259-269.